Supplementary information

A novel exopolysaccharide (p-CY01) from the Antarctic bacterium *Pseudoalteromonas* sp. strain CY01 cryopreserves human red blood cells

Sung Jin Kim,[a, b] Ui Joung Youn,[a] Pilsung Kang,[a] Tai Kyoung Kim,[a] Il-Chan Kim,[a] Se Jong Han,[a] Dong-Woo Lee*[b, c] and Joung Han Yim*[a]

[a]*Division of Polar Life Sciences, Korea Polar Research Institute, Incheon 21990, South Korea.*

[b]*Graduate Program in Biomaterials Science & Engineering, Yonsei University, Seoul 03722, South Korea.*

[c]*Department of Biotechnology, Yonsei University, Seoul 03722, South Korea.*

Correspondence should be addressed to:

Dong-Woo Lee

Department of Biotechnology, Yonsei University, Seoul 03722, South Korea.

E-mail: leehicam@yonsei.ac.kr; Tel: +82-2-2123-2886

Joung Han Yim

Division of Polar Life Sciences, Korea Polar Research Institute, Incheon 21990, South Korea.

E-mail: jhyim@kopri.re.kr; Tel: +82-32-760-5540

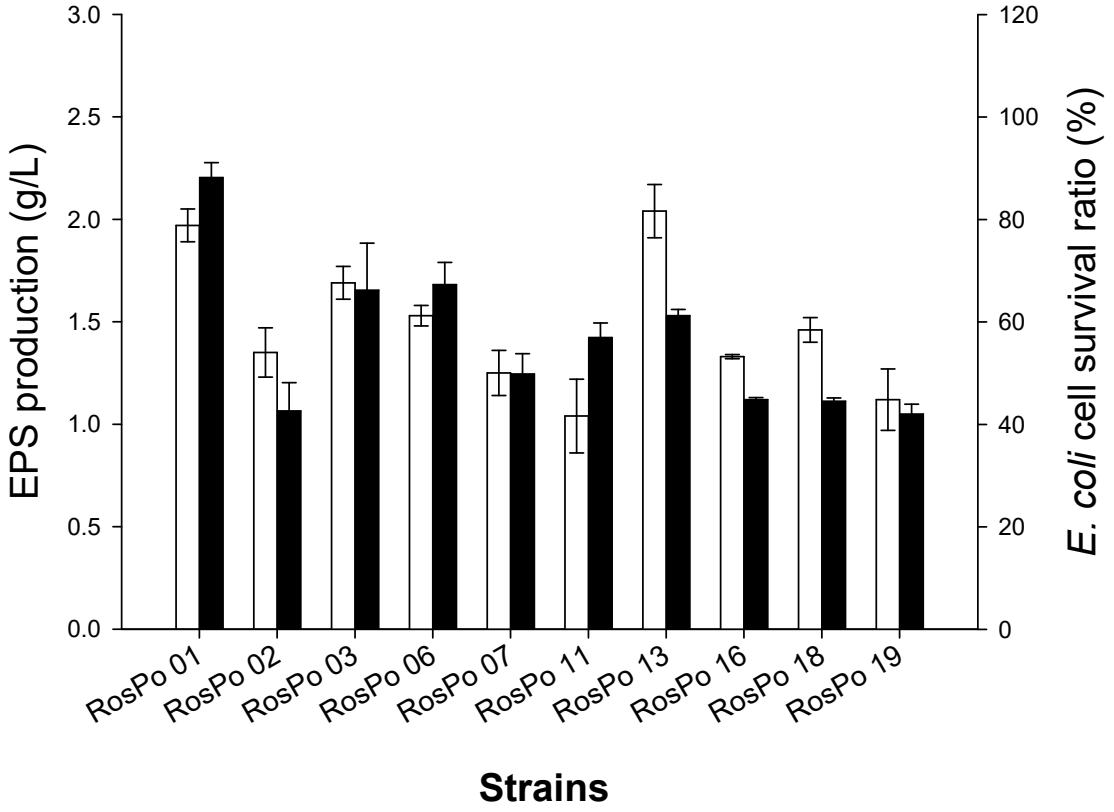

Supplementary Figure S1. Exopolysaccharide (EPS) production and cryoprotective effect on *E. coli*. EPS production was estimated by determining the *E. coli* cell survival ratio after three freeze-thaw cycles in the presence of 0.2% (w/v) crude EPS solutions from the screened strains. The white bar represents EPS production (g/L), and the black bar represents the cryoprotective effect of EPS on *E. coli* (%). The values presented are the mean ± SD from three experimental repeats.

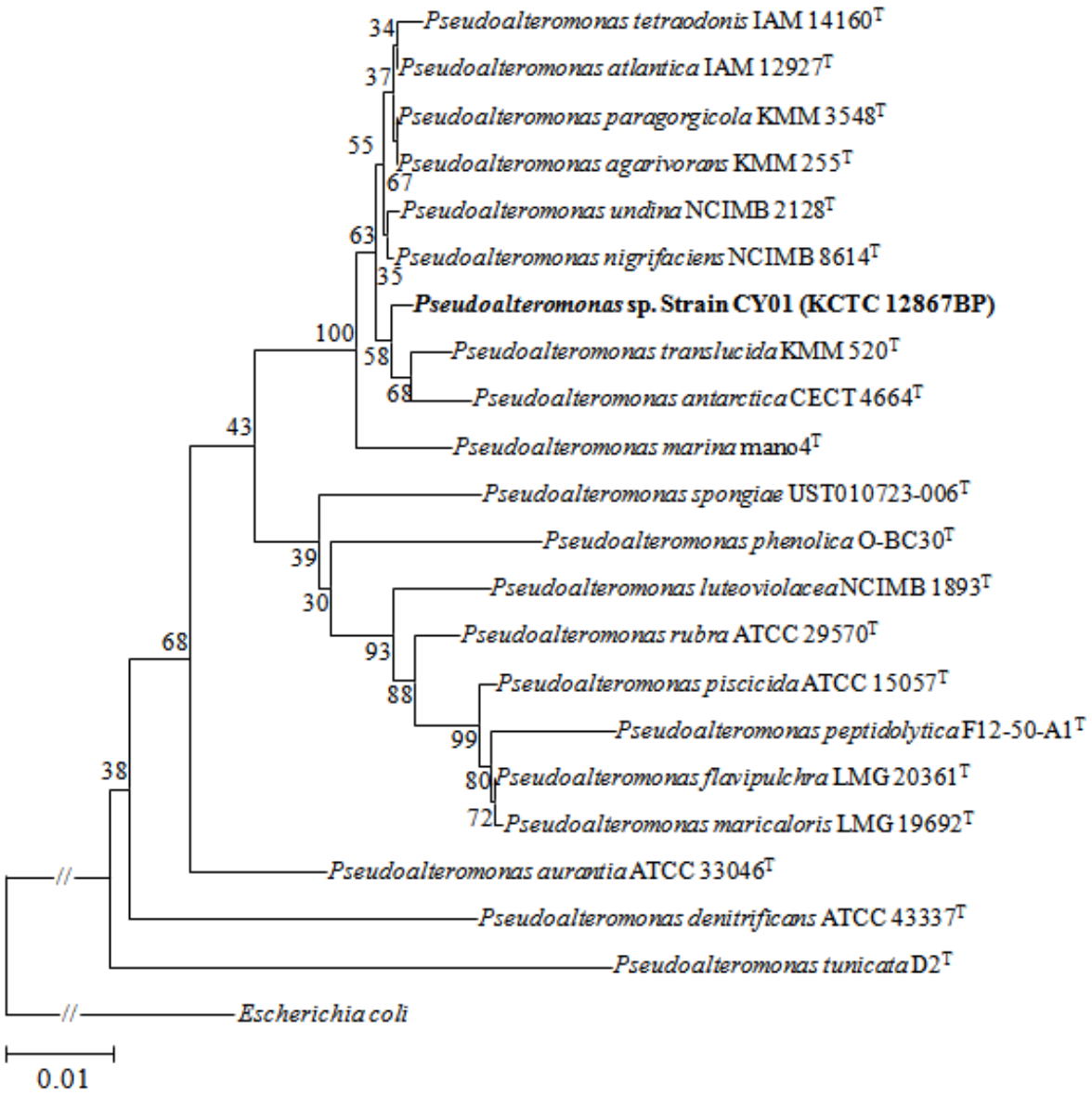

Supplementary Figure S2. The neighbor-joining phylogenetic tree of 16S rRNA sequences. The neighbor-joining tree illustrates the phylogenetic relationship between strain CY01 and closely related *Pseudoalteromonas* strains based on their 16S rRNA sequences. Numbers on nodes indicate the boostrap analysis with 1,000 sequence replicates.

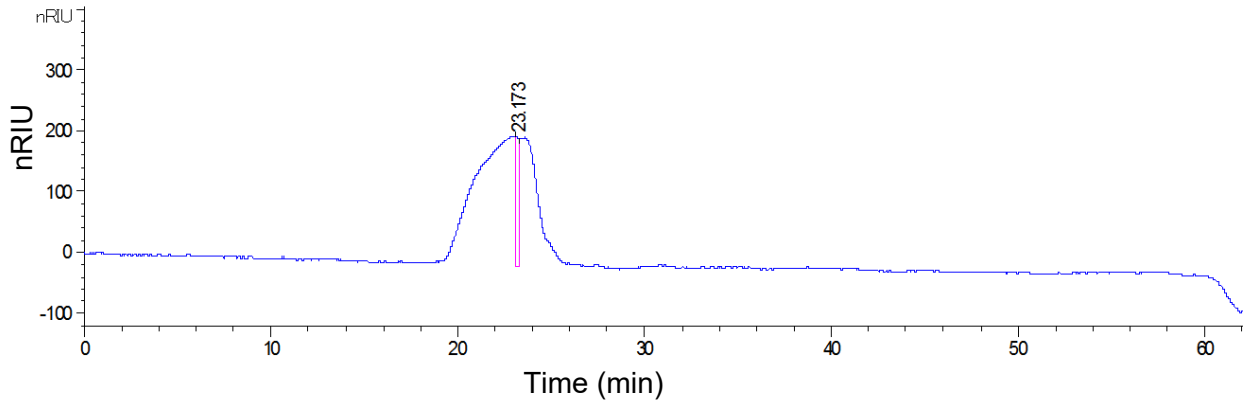

Supplementary Figure S3. Homogeneity analysis of purified EPS from strain CY01 using an Agilent HPLC system. The EPS was dissolved in 0.1M NaCl solution and prepared as 0.1% (w/v) aqueous solutions. Each run process involved injecting 5 µL of the sample solution and monitoring it for 70 min at a flow rate of 0.4 mL min^{-1} at 40°C. The sample was analyzed using an Agilent refractive index detector.

(a)

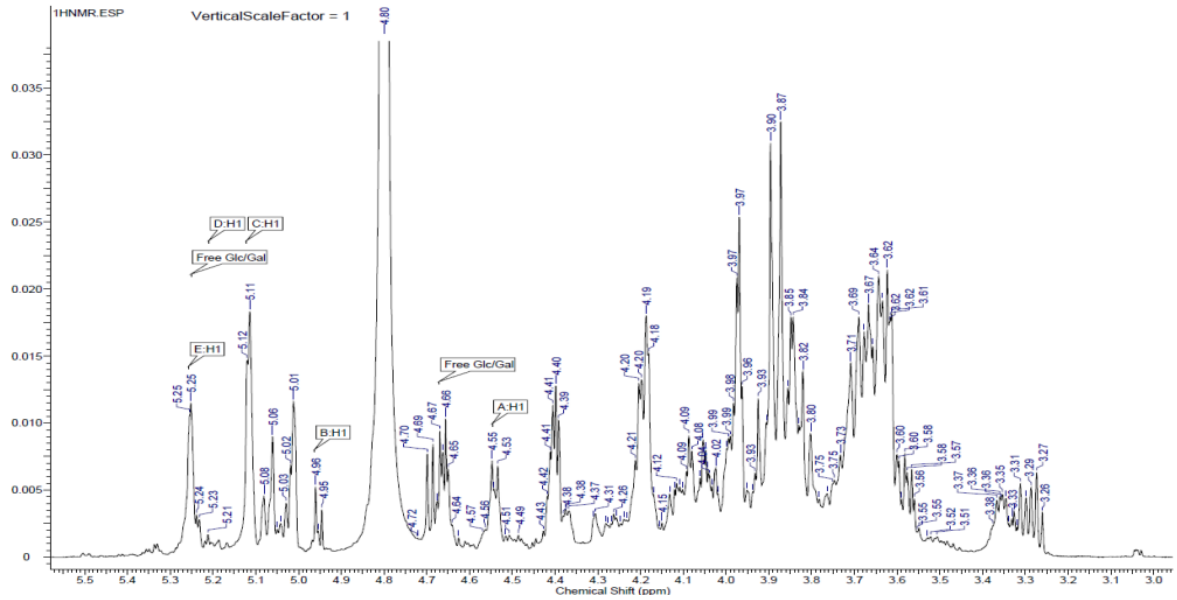

(b)

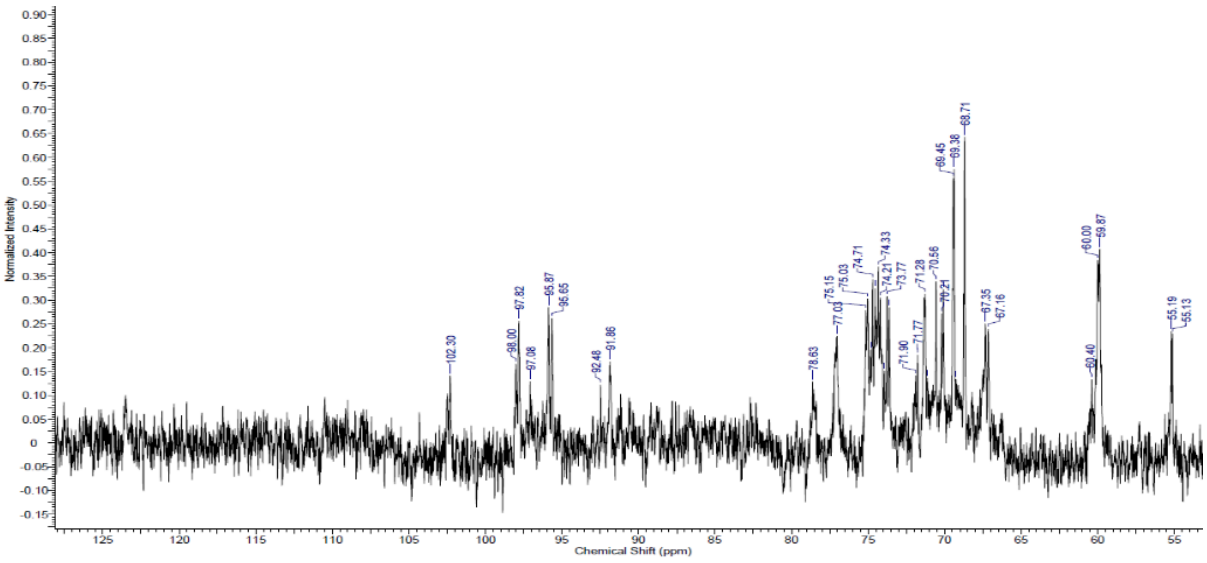

Supplementary Figure S4. ^{1}H and ^{13}C NMR (600 and 150 MHz) spectra of p-CY01 in D_2O (a; ^{1}H NMR, b; ^{13}C NMR)

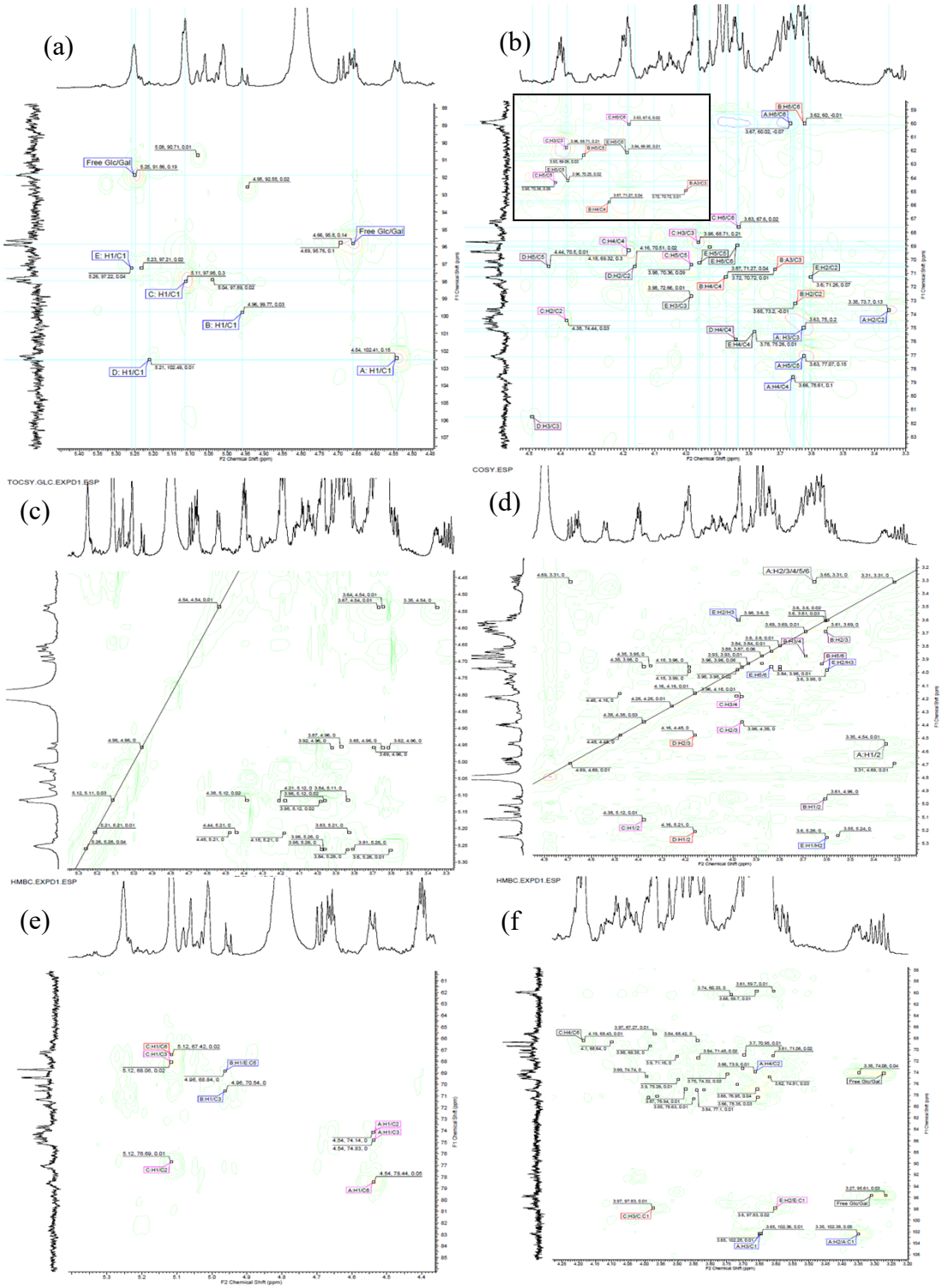

Supplementary Figure S5 Selected parts of HSQC (a) and (b), TOCSY (c), COSY (d), and HMBC (e) and (f) NMR (600 MHz, in D_2O) spectra of p-CY01. The ^1H NMR spectrum of p-CY01 showed anomeric proton signals at δ_H 4.54 (d, $^3J_{1,2}$ = 8.4 Hz) and at δ_H 4.95 (br s) to 5.23 (br s) ppm, indicating a β-glycosidical ($^3J_{1,2}$ = ≈ 8.0 Hz) and α-glycosidical ($^3J_{1,2}$ = < 3.0 Hz) configurations, respectively. The NMR

and ^{1}H-^{13}C HSQC spectra of p-CY01 displayed five characteristic sugar residues at δ_H 4.54/δ_C 102.4, 4.96/99.7, 5.12/97.9, 5.21/102.4, and 5.26/97.2 ppm, labeled as **A**, **B**, **C**, **D**, and **E**, respectively (Supplementary Table S1 and Supplementary Fig. S3), along with free sugar units at δ_H 4.66/δ_C 95.8 and 5.25/91.8, respectively, corresponding to the signals of *β*-D-Glc*p*/-D-Gal*p* and *α*-D-Glc*p*/-D-Gal*p*. The ^{1}H-^{13}C HSQC, ^{1}H-^{1}H TOCSY, including a selective TOCSY method, and ^{1}H-^{1}H COSY experiments established their related proton and carbon residues (Supplementary Table 1), assigned as **A**: →4)-*β*-D-Glc*p*-(1→,[1,2] **B**: Terminal-*α*-D-Glc*p*-(1→, [3-5] **C**: →6)-*α*-D-Gal*p*-(1→, [6] **D**: →3,4)-*α*-D-Gal*p*-(1→, [7,8] and **E**: →4,6)-*α*-D-Glc*p*-(1→, [9] respectively (Supplementary Table S1 and Supplementary Fig. S4). These were in good agreement with the results of the GC-MS analysis. However, signals for the remaining terminal-galactose unit were hardly distinguishable in the 1D and 2D NMR analyses. The ^{1}H-^{13}C HMBC and ^{1}H-^{1}H NOESY analyses support linkages between sugar residues since the methods display clear and strong correlations between sugar units. In the residue **A**, a major backbone of this polysaccharide, a strong correlation peak from the anomeric proton (H-1) to the downfield shifted carbon signal at δ_C 78.6 (C-4) and weak cross peaks with C-2/C-3 were observed in HMBC spectrum, indicating a main repeating unit of p-CY01 as shown in Supplementary Fig. S4 and Fig. S5. [1, 2]

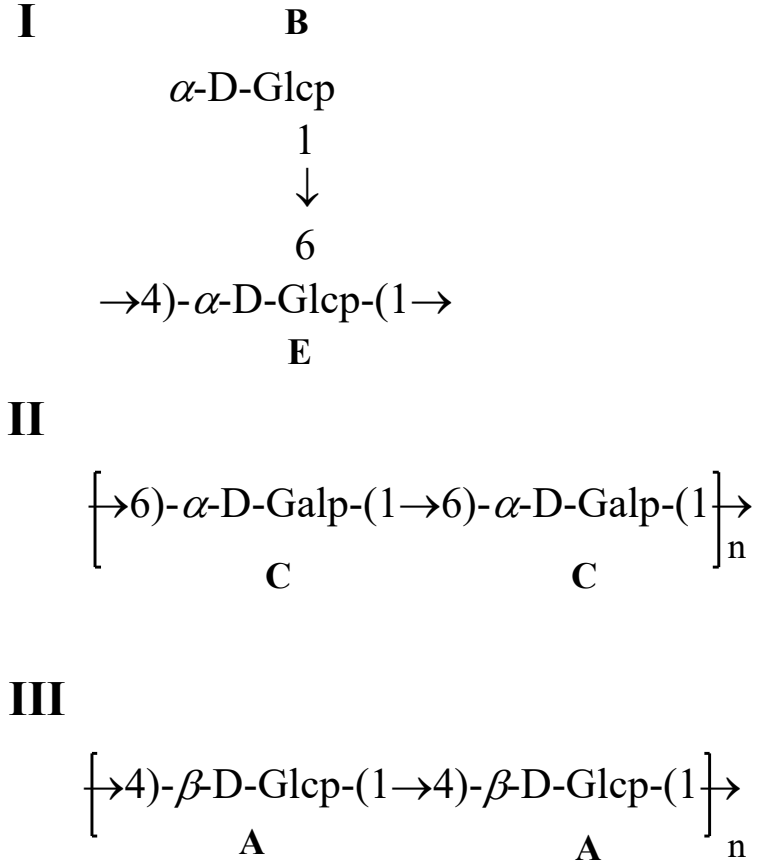

Supplementary Figure S6 Structure of the predominant repeating units and proposed partial structures of the *O*-polysaccharide of p-CY01.

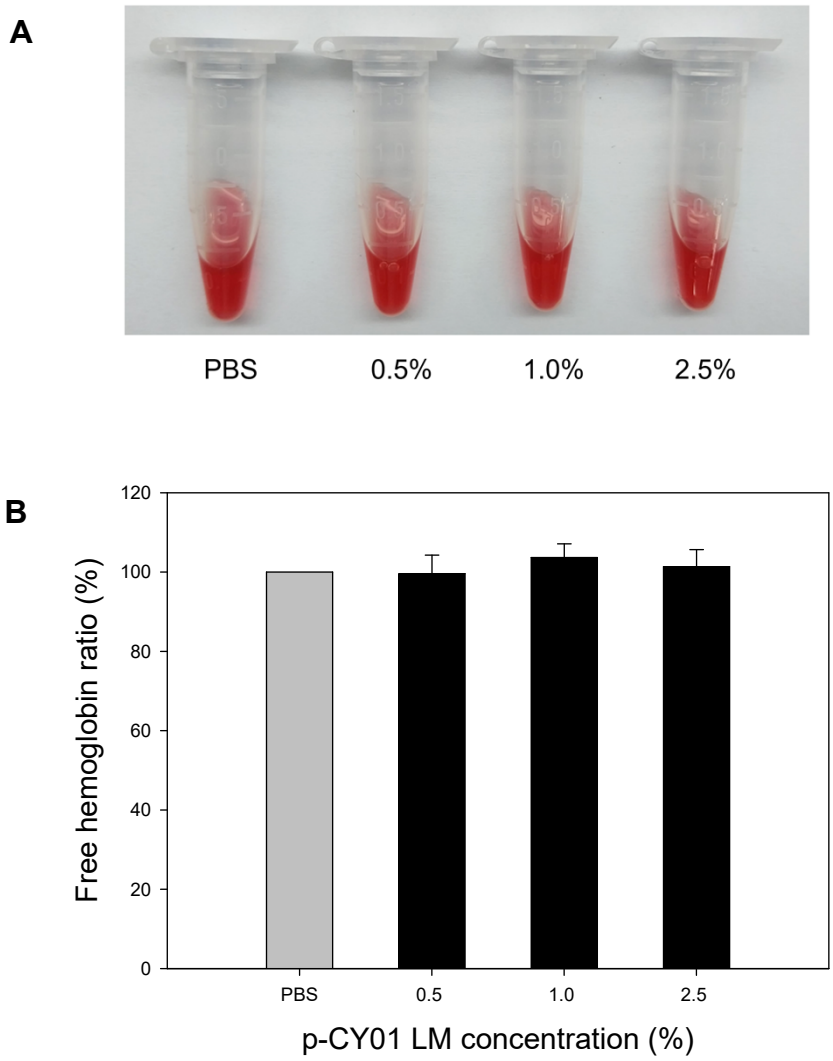

Supplementary Figure S7. Confirmation of interaction between p-CY01 LM and free hemoglobin resulting in precipitated hemoglobin. (A) No decrease in hemoglobin pigment was observed based on p-CY01 LM concentration when compared to PBS. (B) Quantitative measurement of the free hemoglobin ratio using Drabkin's method revealed that even with an increase in hemoglobin concentration, precipitated hemoglobin was not generated when using p-CY01 LM. The value remained comparable to the free hemoglobin ratio in PBS. The presented values represent means ± standard deviation from three experimental replicates.

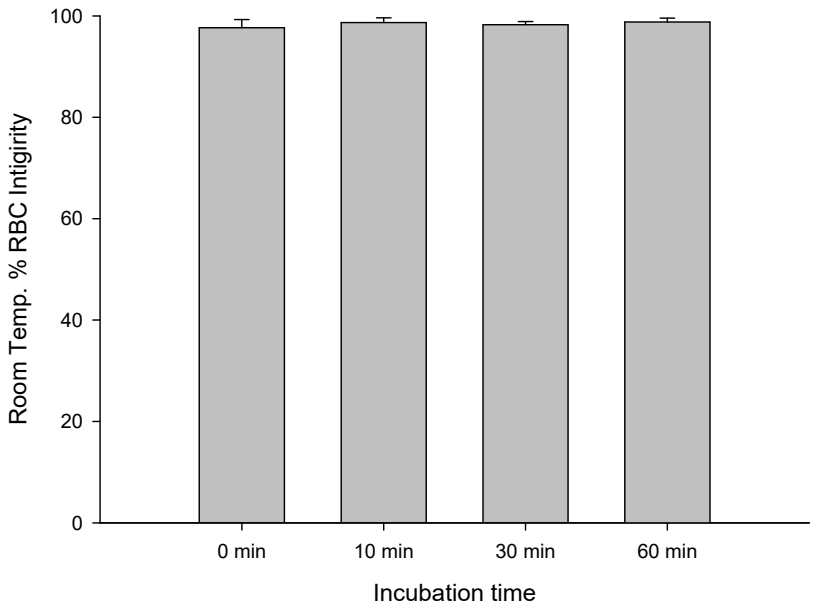

Supplementary Figure S8. Biocompatibility of p-CY 01 LM solution (2.5% (w/v) p-CY 01 LM with 1% (v/v) Glycerol and DMSO in ADSOL) on the RBC. RBC integrities after room temperature incubation for an indicated time without freezing. Haemolysis was quantified using Drabkin's assay to determine % RBC integrity (100 - % hemolysis). The values shown are means ± standard deviation from three experimental replicates.

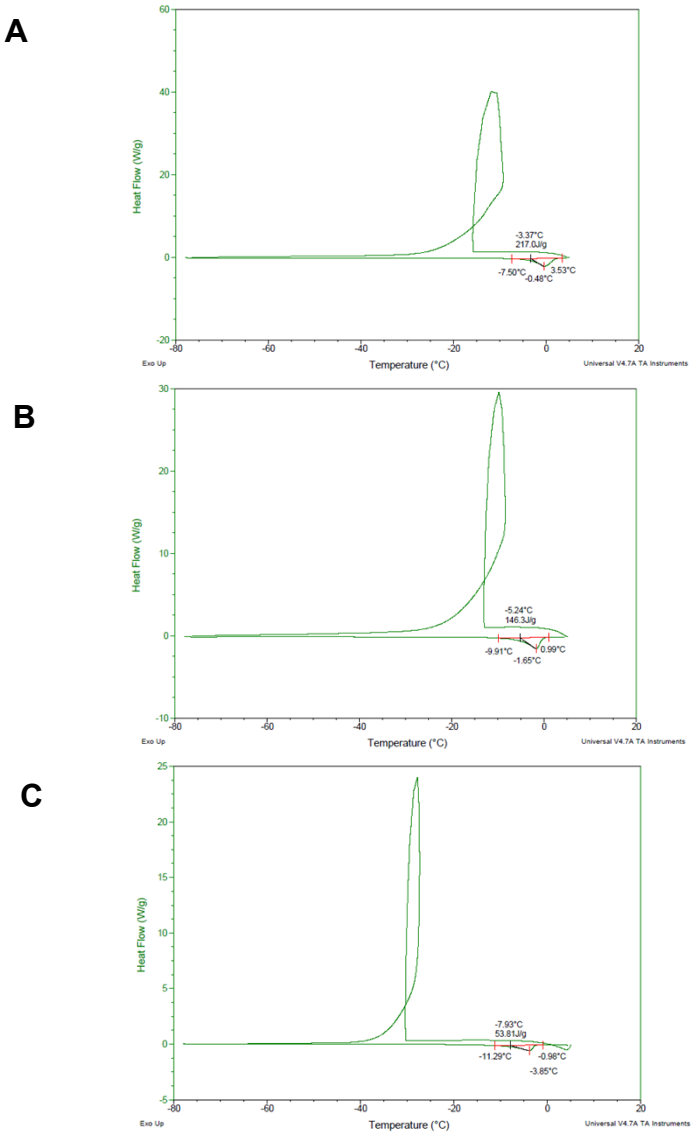

Supplementary Figure S9. Differential scanning calorimetry (DSC) analysis of p-CY01 LM solutions. Samples were individually cooled from +5 °C to −78 °C at a rate of 40 °C min^{-1} and thawing at 2°C min^{-1}. (A) 1% Glycerol (v/v) and 1% DMSO (v/v) were used as a negative control. (B) 1% Glycerol (v/v), 1% DMSO (v/v) and 0.5% p-CY01 LM (w/v). (C) 1% Glycerol (v/v), 1% DMSO (v/v) and 2.5% p-CY01 LM (w/v). The supercooling points of (A) 1% Glycerol (v/v) and 1% DMSO (v/v) were used as a negative control, (B) 1% Glycerol (v/v), 1% DMSO (v/v) and 0.5% p-CY01 LM (w/v) and (C) 1% Glycerol (v/v), 1% DMSO (v/v) and 2.5% p-CY01 LM (w/v) were −14.9 °C, -13.8 °C and −30.5 °C, respectively.

Supplementary Table 1. ^{1}H and ^{13}C NMR (600 and 150 MHz, in D_2O) data for the residues **A** to **E** from p-CY01.

Residues	H-1 C-1	H-2 C-2	H-3 C-3	H-4 C-4	H-5 C-5	H-6 C-6
A: →4)-*β*-D-Glc*p*- (1→	4.54 102.4	3.35 73.7	3.64 75.0	3.66 78.6	3.64 77.0	3.67 60.0
B: T-*α*-D-Glc*p*- (1→	4.96 99.7	3.61 73.2	3.69 70.6	3.87 71.2	3.93 69.0	3.62 60.0
C: →6)-*α*-D-Gal*p*- (1→	5.12 97.9	4.38 74.4	3.96 68.7	4.18 69.3	3.98 69.2	3.83 67.6
D: →3,4)-*α*-D- Gal*p*-(1→	5.21 102.4	4.16 70.5	4.48 81.5	3.84 75.8	4.44 70.5	- -
E: →4,6)-*α*-D- Glc*p*-(1→	5.26 97.2	3.60 71.2	3.98 72.6	3.80 75.2	3.96 70.2	3.84 68.9

Supplementary Table 2. Statistical analysis of cryo-additives using Plackett-Burman design.

Variables	Effect	S.E.	*t*-statistics	*P*-value
Glycerol	2.321	0.9096	1.28	0.224
DMSO	2.621	0.9096	1.44	0.173
ADSOL	5.826	0.9096	3.20	0.007
p-CY01 LM	51.694	0.9096	28.41	0.000

References

1. Colquhoun, I.J.; Defernez, M.; Morris, V.J. NMR studies of acetan and the related bacterial polysaccharide, CR1/4, produced by a mutant strain of *Acetobacter xylinum*. *Carbohydr Res* **1995**, *269*, 319-331.
2. Robijn, G.W.; Gutiérrez Gallego, R.; van den Berg, D.J.C.; Haas, H.; Kamerling, J.P.; Vliegenthart, J.F.G. Structural characterization of the exopolysaccharide produced by *Lactobacillus acidophilus* LMG9433. *Carbohydr Res* **1996**, *288*, 203-218.
3. Zheng, C.; Dong, Q.; Chen, H.; Cong, Q.; Ding, K. Structural characterization of a polysaccharide from *Chrysanthemum morifolium* flowers and its antioxidant activity. *Carbohydr Polym* **2015**, *130*, 113–121.
4. Li, B.; Dobruchowska, J.M.; Hoogenkamp, M.A.; Gerwig, G.J. Structural investigation of an extracellular polysaccharide produced by the cariogenic bacterium *Streptococcus mutans* strain UA159. *Carbohydrate Polym* **2012**, *90*, 675–682.
5. Mandal, E.K.; Maity, K.; Maity, S.; Gantait, S.K.; Behera, B.; Maiti, T.K.; Sikdar, S.R.; Islam, S.S. Chemical analysis of an immunostimulating (1→4)-, (1→6)-branched glucan from an edible mushroom, *Calocybe indica*. *Carbohydr Res* **2012**, *347*, 172–177.
6. Marshall, V.M.; Dunn, H.; Elvin, M.; McLay, N.; Gu, Y.; Laws, A.P. Structural characterization of the exopolysaccharide produced by *Streptococcus thermophilus* EU20. *Carbohydr Res* **2001**, *331*, 413–422.
7. Fontana, C.; Li, S.; Yang, Z.; Widmalm, G. Structural studies of the exopolysaccharide from *Lactobacillus plantarum* C88 using NMR spectroscopy and the program CASPER. *Carbohydr Res* **2015**, *402*, 87–94.
8. Petersen, B.O.; Hindsgaul, O.; Paulsen, B.S.; Redondo, A.R.; Skovsted, I.C. Structural elucidation of the capsular polysaccharide from *Streptococcus pneumoniae* serotype 47A by NMR spectroscopy. *Carbohydr Res* **2014**, *386*, 62–67.
9. Li, B.; Dobruchowska, J.M.; Gerwig, G.J.; Dijkhuizen, L.; Kamerling, J.P. Structural investigation of water-soluble polysaccharides extracted from the fruit bodies of *Coprinus comatus*. *Carbohydr Polym* **2013**, *91*, 314– 321.